

Bonding in the trihalides (X_3^-), mixed trihalides (X_2Y^-) and hydrogen bihalides (X_2H^-). The connection between hypervalent, electron-rich three-center, donor-acceptor and strong hydrogen bonding ‡

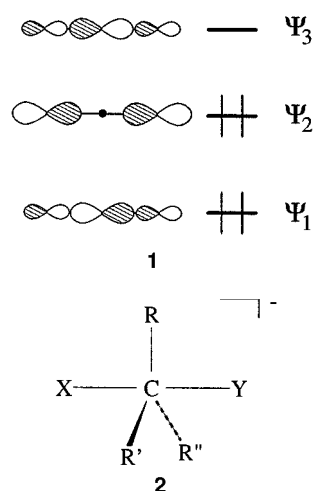
Gregory A. Landrum, Norman Goldberg*† and Roald Hoffmann*

Department of Chemistry and Materials Science Center, Cornell University, Ithaca, New York, 14853-1301, USA

The nature of the bonding in the trihalides (X_3^-), mixed trihalides (X_2Y^-), and hydrogen bihalides (X_2H^-) has been analysed by applying ideas from qualitative molecular orbital theory to computational results from density-functional calculations. A systematic, unified investigation showed that the bonding in all of these diverse anions can be understood in terms of the Rundle–Pimentel scheme for electron-rich three-center bonding. It also showed the equivalence of the donor-acceptor and hypervalent bonding views of these molecules. Less symmetrical trihalide ions were studied as well, *e.g.* the reasons why $IICl^-$ is favored over $IClI^-$ were explored. This site preference is considerably less pronounced in the $I^-I\text{Br}$ system. The donor-acceptor perspective (X^- attack at the two possible sites of $X-Y$) was found to be useful. Similarly, formation of XHX^- from X^- and HX is strongly favored over formation of XXH^- , and the energy difference between these two geometries increases with increasing electronegativity of X .

The nature of the chemical bonding in hypervalent molecules, species with main group atoms that violate the octet rule, has long posed an enigma. In early attempts to explain the stability of molecules such as I_3^- , SF_6 and PCl_5 by means of the valence-bond method, Pauling and others^{1,2} postulated the participation of d orbitals on the central atom. More than 40 years ago, in their seminal publications on the bonding in the triiodide anion, I_3^- , Pimentel³ and Rundle⁴ independently proposed an alternative explanation. The Rundle–Pimentel scheme invokes delocalized three-center σ bonding as shown in **1**: three p orbitals combine to give one bonding, one non-bonding and one antibonding molecular orbital; the lower-lying two orbitals are occupied. This scheme, elaborated in various ways, remains the basis of the generally accepted ‘electron-rich three-center bonding’ view of hypervalency. Pimentel³ proposed a similar scheme to account for the bonding in the hydrogen-bridged bihalide anions, XHX^- ($X = F, Cl, Br$ or I), species that are known to possess exceptionally strong ‘hydrogen bonds’.

Since these seminal contributions were published numerous theoretical studies on the nature of the bonding in hypervalent molecules have been carried out.^{5–18} The need for a more detailed energetic decomposition of interactions between closed-shell species became apparent 40 years ago, when Coulson¹⁹ examined the hydrogen bonding in FHF^- with a simple electrostatic model. He concluded that a purely electrostatic interaction cannot account for the bonding of this species. Coulson thus introduced a bond-partitioning scheme that divided the attractive forces between interacting fragments into four major components: electrostatic, covalent, repulsive and dispersion forces. Twenty years later Morokuma and co-workers^{20–23} extended this approach to study the interactions between molecules within Hartree–Fock theory and a similar *ansatz* has recently been used within a Natural Bond Order analysis.^{24,25} When Morokuma and co-workers²³ applied their analysis to investigate the bonding in FHF^- they found that



although there are strong electrostatic forces that hold the anion together, there are also significant charge-transfer contributions to the attractive forces between a HF molecule and a fluoride anion F^- .

In this contribution we examine the bonding of the homoatomic trihalide anions, X_3^- , some mixed trihalides, X_2Y^- , and the hydrogen bihalide anions, XHX^- , using density-functional theory and qualitative orbital analysis. Our goal is to understand the various interactions responsible for the bonding between the neutral and anionic closed-shell fragments that compose these anions. We also seek to obtain an understanding of the changes in the bonding of these triatomics upon moving from homoatomic to mixed anions. Using the concept of an electronegativity perturbation, we will attempt to provide a unified picture of the bonding in these species.

Further motivation for study of the trihalides is provided by the fact that their bonding is similar to that of the transition-state structure of one of the most important reactions in organic chemistry, the S_N2 reaction (for a recent theoretical monograph on the S_N2 mechanism, see ref. 26 and refs. therein). This reaction is known to proceed *via* a transition state (see **2**) in which the attacking nucleophile X^- , the central carbon atom,

† Present address: Institut für Organische Chemie, TU Braunschweig, Hagenring 30, D-38106 Braunschweig, Germany.

‡ Non-SI units employed: cal = 4.184 J, eV \approx 1.60 \times 10⁻¹⁹ J, D \approx 3.33 \times 10⁻³⁰ C m.

and the leaving group Y are arranged in a linear fashion. Thus, the structure of the S_N2 transition state and the number of electrons intimately involved in the reaction correspond to a three-center four-electron species. While this linear geometry is an energy minimum for the trihalides, for carbon it is a transition state due to the strong endothermicity associated with bending the three substituents out of their positions at the three corners of a tetrahedron and into a planar arrangement.²⁶ Upon moving down Group 14 from carbon, however, stable, five-co-ordinate species with geometries like **2** are well known.

We also have strong reason to believe that the bonding in both R_2QX_2 ($Q = \text{Se or Te}$; $X = \text{I, Br or Cl}$)^{27–30} and R_3PX_2 ($X = \text{I, Br or Cl}$)^{31–35} complexes, where there are pseudo-linear XQX or QXX units, can be well understood in terms of an electronegativity perturbation of an X_3^- anion.³⁶ Here we will lay a theoretical foundation which can then be built upon in future studies of these and other molecules exhibiting electron-rich three-center bonding.

Computational Methodology

The calculations were carried out using the Amsterdam Density Functional (ADF) program.^{37–39} Gradient corrections were performed using the Becke (exchange)^{40,41} and Perdew (correlation)^{42,43} formulations. The valence atomic orbitals were represented using a basis set of Slater type orbitals (STOs). Triple- ζ basis sets (three STOs per atomic orbital, AO) with one polarization function were used for the halides. A triple- ζ basis set with two added polarization functions was used for hydrogen.⁴⁴ The core orbitals of the halides were frozen out to 1s (F), 2p (Cl), 3p (Br) and 4p (I).³⁷

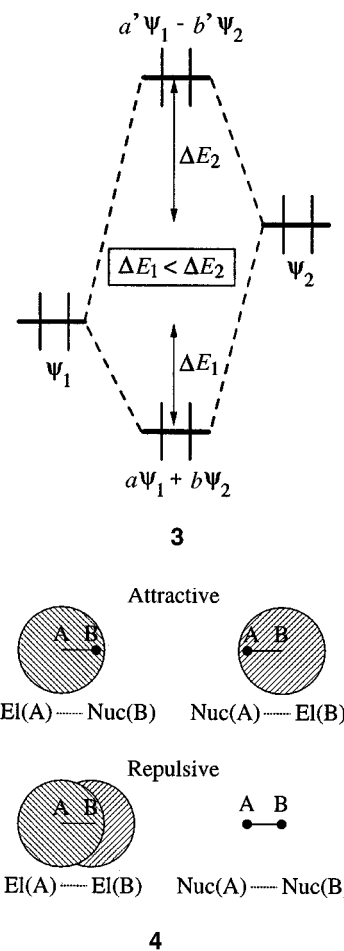
Unless otherwise stated, all bonding energies we report include both zero-point energy (ZPE) and basis set superposition error (BSSE) corrections and are referenced to the optimized geometries of the fragments that compose the molecule. The BSSE corrections were applied using the method of Rosa *et al.*⁴⁵ Frequency calculations were performed on all optimized geometries to ensure that they are true minima. Reported charges were calculated using the Hirshfeld analysis,⁴⁶ as the more familiar Mulliken analysis is known to be unreliable when large basis sets are used. Geometry optimizations were carried out in $C_{\infty v}$ symmetry and started from asymmetric structures in order to allow optimization to an asymmetric geometry.

The contour plots of molecular orbitals from ADF were generated using a modified version of VIEWKEL, a part of YAEHMOP.⁴⁷ These plots contain contributions from both the valence and core functions (which can be seen in the regions near the atomic nuclei in each plot). All contour plots use the same contour levels: $-0.10, -0.08, -0.06, -0.04, -0.02, 0.02, 0.04, 0.06, 0.08$ and 0.10 .

Within ADF, bonding energies between fragments of a molecule are decomposed using the Transition State (TS) procedure of Ziegler.⁴⁸ This scheme breaks interaction energies down into three chemically intuitive contributions: Pauli repulsion, electrostatic attraction, and orbital interactions. The procedure has been described in great depth in ref. 48 and refs. therein; here we provide a short overview of the contributions to the various energy terms.

The first two terms in the energy decomposition (Pauli repulsion and the electrostatic) can be calculated based solely upon interactions between the charge densities of the unperturbed fragments. The Pauli repulsion (also called exchange repulsion or overlap repulsion) is the counterpart of four-electron two-orbital interactions in qualitative molecular orbital theory,⁴⁹ **3**. This familiar destabilization is caused by the larger energy shifts of antibonding orbitals compared to bonding orbitals.

The four major contributions to the electrostatic energy term are shown schematically in **4**. In most cases the attractive interactions between the electron clouds of one fragment and the nuclei of the other are stronger than the sum of the electron–



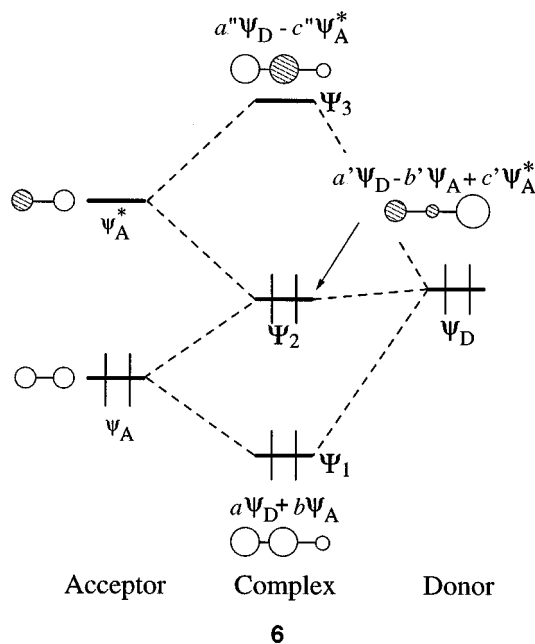
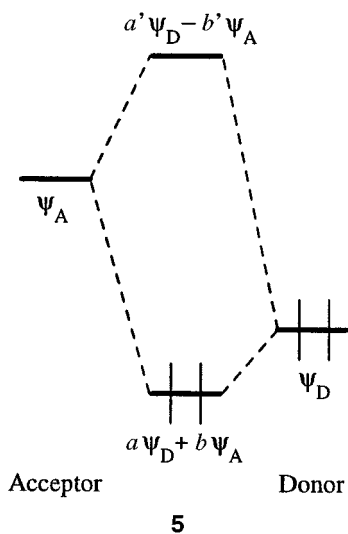
electron and nuclear–nuclear repulsions; thus the net electrostatic interaction is attractive.

The orbital interaction energy within the Transition State method is calculated after the SCF (self-consistent field) iterations have been completed. This energy term arises due to mixing of occupied and unoccupied orbitals. The mixing gives rise to charge transfer between fragments (this will be very important in our discussion of donor–acceptor interactions) and polarization within the fragments. The orbital interaction energy is stabilizing, since the destabilizing orbital interactions (arising from two-orbital four-electron interactions) have already been accounted for in the Pauli repulsion term. Within ADF it is possible to decompose the orbital interaction energy by symmetry species. This symmetry decomposition will be used to determine which orbital contributions are most important for the bonding.

The total bonding energy between the fragments used in an ADF calculation is determined by the sum of the Pauli repulsion, electrostatic attraction, and orbital interaction terms. While it has been the custom in reporting results from ADF to combine the Pauli and electrostatic terms into a so-called ‘steric repulsion’ term, we will adopt a slightly different approach. We choose to sum the Pauli and orbital energy terms to give a ‘net orbital interaction energy’. This is due to our bias towards seeing things in terms of orbital interactions. Conceptually, we think of the Pauli terms, arising mainly from two-orbital four-electron interactions, as part of the net orbital interaction in a molecule.

Donor–Acceptor Interactions

Since our approach to describing the interactions in the trihalides will be using the concepts of donor–acceptor bonding, it is useful quickly to review the essentials of this type of interaction. A donor–acceptor (or dative) bond is generally viewed



as arising from an interaction between a relatively high-lying doubly occupied orbital on the donor fragment and a low-lying empty orbital on the acceptor fragment. A sketch of the energy-level diagram for a simple two-level donor-acceptor interaction is shown in 5. Here the LUMO (lowest unoccupied molecular orbital) of the acceptor (ψ_A) mixes in a bonding way with the HOMO (highest occupied molecular orbital) of the donor (ψ_D) to form the HOMO of the complex. Significant charge transfer from the donor to the acceptor, through the partial occupation of ψ_A results. The stabilization of the HOMO of the composite complex relative to the position of ψ_D determines the strength of the donor-acceptor bond.

However, in the majority of the three-center systems we will discuss, the donor-acceptor interaction is more complicated, since the acceptor also has occupied levels which need to be considered. This leads to a three-level problem, generically sketched in 6. Here the composite orbital Ψ_1 is made up of the HOMO of the acceptor (ψ_A) with a small contribution from the HOMO of the donor (ψ_D). This orbital is bonding between the two fragments. The HOMO of the complex (Ψ_2), primarily centered on the donor, with smaller contributions from both ψ_A and ψ_A^* , determines the net bonding character of the donor-acceptor interaction. If the amount of ψ_A^* mixing is small, then Ψ_2 may be strongly antibonding between the fragments, due to the antibonding mixing with ψ_A . This destabilization could outweigh the bonding contributed by Ψ_1 , and the complex may

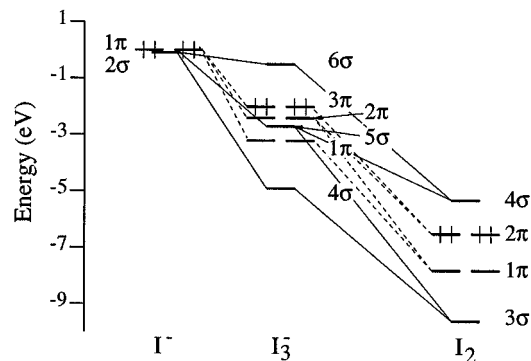


Fig. 1 Fragment molecular orbital interaction diagram for I_3^- . The symmetry labels given are appropriate for the C_{3v} symmetry within which the calculation was performed. Solid lines connect levels of σ symmetry, dashed lines connect levels of π symmetry

well be unstable. On the other hand, a sizable admixture of ψ_A^* into Ψ_2 will stabilize the complex by reducing the antibonding component between the donor and acceptor. The above discussion focuses on first-order (in the wavefunctions) mixing; second-order mixing will produce polarization at the acceptor in Ψ_1 and Ψ_2 , *i.e.* a mixing of these two orbitals.⁴⁹

Formation of such a donor-acceptor bond leads to a number of changes in the electronic structure of the fragments. First, there is a net transfer of electrons from the donor to the acceptor. The acceptor gains electrons *via* the mixing of ψ_A^* (which is unoccupied in the free acceptor) into the HOMO of the complex. The donor loses electrons because of the mixing of ψ_D into the unoccupied, donor-acceptor antibonding MO Ψ_3 . Secondly, the partial occupation of ψ_A^* , which is antibonding within the acceptor, weakens the bonding in the acceptor. The stronger the donor-acceptor interaction, the larger these perturbations will be.

By using this donor-acceptor language in our discussion of the bonding within the trihalides and hydrogen dihalides, we will show in the sequel the similarities between what is usually called hypervalent bonding, electron-rich three-center bonding, strong hydrogen bonding, and donor-acceptor interactions.

The Electronic Structure and Bonding of X_3^-

We begin our discussion with the homoatomic trihalide anions X_3^- ($X = F, Cl, Br$ or I), analysing these well studied molecules in terms of the bonding of an X^- to X_2 . We start with an in-depth analysis of I_3^- and then summarize the results for the other trihalides.

The optimized geometry computed for I_3^- was a symmetric (D_{3h}) molecule with I-I distances of 3.14 Å. While the geometry of I_3^- in the gas phase is not experimentally known, this bond length falls within the wide range observed in the solid state.⁵⁰ The I^-I_2 bonding energy was calculated to be 37.5 kcal mol⁻¹.§ The two terminal iodines have charges of -0.419, compared with a charge of -0.163 on the central atom. This charge distribution is easily explained within the qualitative orbital scheme sketched earlier (1), where the largest contributors to the HOMO are the terminal atoms.

To help us understand the bonding in I_3^- in more detail, a Fragment Molecular Orbital (FMO) interaction diagram for the formation of I_3^- from I^- and I_2 is shown in Fig. 1. A quick note for readers who are used to seeing the FMO diagrams that come out of the extended Hückel method is in order. The orbitals of the I^- fragment are quite high in energy relative to those of I_2 , and the I_3^- levels come somewhere in between. This

§ To ensure that our results were not inaccurate due to neglect of relativistic effects, calculations were carried out on I_3^- using the scalar relativistic option within ADF. The differences between the geometry and I^-I_2 binding energy were deemed to be chemically insignificant.

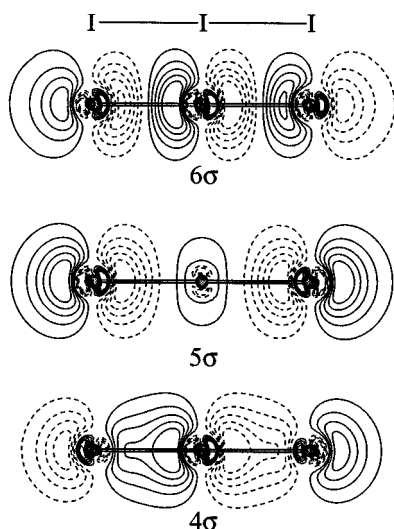


Fig. 2 The σ MOs in the vicinity of the HOMO of I_3^-

is a bit disconcerting at first, but is physically reasonable when we remember that these calculations include electron–electron repulsion effects (omitted in the more common one-electron interaction diagrams). The binding energies of electrons in anions are known from photoelectron spectroscopy to be lower (*i.e.* the orbitals are higher in energy) than those in the corresponding neutrals.⁵¹ We are just seeing this effect in the results of the density functional calculation. Notice also that the levels drop down in energy when the negative charge is delocalized over three atoms in I_3^- .

The numbering of the energy levels in Fig. 1 neglects the 4d levels which were included in the valence orbital basis set for iodine. These levels do not play a large role in the bonding and we will not be spending any time discussing them. The resulting numbering scheme is consistent with what would come out of an extended Hückel calculation with just the I 5s and 5p orbitals included in the basis set.

The energy level diagram for I_3^- in the center of Fig. 1 is perfectly reasonable within the framework of qualitative MO theory. The π system of I_3^- is completely full (the bonding, non-bonding, and antibonding π orbitals, coming in degenerate pairs, are all occupied) and the σ system has two of three orbitals occupied. We now take a closer look at that σ system of I_3^- .

If we examine the MOs of the complex (I_3^-), Fig. 2, we see that they bear a comforting resemblance to those sketched in our introduction (1). The highest occupied σ orbital of I_3^- , 5 σ , is the important middle orbital of the three-orbital donor–acceptor interaction we discussed earlier. In this case, enough of the LUMO of the acceptor mixes in almost completely to remove the contribution on the middle I. This is a consequence of the symmetry of this D_{nh} molecule: actually, there can be no admixture of p_{σ} (which is of σ_u symmetry in D_{nh}) on the central atom in a σ_g MO.

Now let us look at the I_3^- orbitals as arising from an I^- – I_2 donor–acceptor interaction. The major σ FMOs of I_3^- are the 3 σ (which is I–I bonding) and 4 σ (the I–I antibonding LUMO) of I_2 and the p_{σ} orbital of I^- . The 3 σ and 4 σ frontier orbitals of I_2 are shown in Fig. 3. In I_3^- , I^- acts as the donor and I_2 as the acceptor. The important acceptor orbital on I_2 is the LUMO: 4 σ . The extent of the mixing of this MO into occupied levels can be seen quite clearly in the orbital breakdown: the 5 σ orbital of I_3^- is 26% I_2 3 σ , 24% I_2 4 σ and 48% I^- p_{σ} . We will soon see that the percent contribution of the acceptor LUMO to the highest occupied σ orbital of the complex (Ψ_2 in 6) as well as the total occupation of the acceptor LUMO will provide a measure of the strength of the orbital component of the donor–acceptor interaction.

We next examine the decomposition of the I^- – I_2 interaction

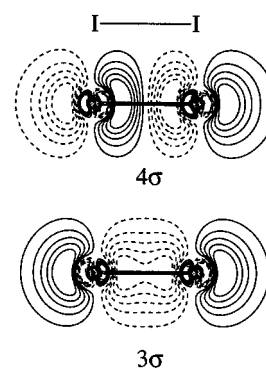


Fig. 3 The important valence σ orbitals of I_2 : 3 σ , the highest occupied orbital in the σ system and 4 σ , the LUMO of the molecule

energy. Before proceeding, however, it is essential to point out that the summed interaction energy that is discussed here is not the same as the bonding energy reported above. The bonding energy includes a number of terms (zero point energy, ‘preparation energy’ of the I_2 fragment, BSSE corrections, *etc.*) which we will not interpret here.

In this interaction between closed-shell species the Pauli repulsion energy is a quite substantial 51.4 kcal mol⁻¹. While, unfortunately, ADF does not provide a symmetry decomposition of the Pauli repulsion, it is reasonable to assume that a significant fraction of this arises from the full π system of I_3^- . The favorable orbital interaction energy, –55.8 kcal mol⁻¹, is almost entirely a result of the σ interactions, which contribute –53.7 kcal mol⁻¹. This can be easily understood if one considers that σ is the only symmetry species for which there exists a low-lying unoccupied orbital which can be mixed in to stabilize what is otherwise a closed shell–closed shell interaction. The π system is, as mentioned above and shown in Fig. 1, completely full. The net orbital energy (recall that we define this as the sum of the Pauli and orbital interaction terms) is only –4.4 kcal mol⁻¹.

The last contribution to the interaction energy between I^- and I_2 is the electrostatic term, which provides 44.3 kcal mol⁻¹ of stabilization to the complex. This number seems a little large until we remember that this is not the interaction energy of a point negative charge with a neutral molecule. As it is defined in the energy partitioning scheme we use, the electrostatic energy includes terms such as the interaction between the electron cloud on one fragment with the nuclei of the other. The orbitals of I are quite diffuse, and so these interactions are significant, even at an I–I separation of more than 3.0 Å.

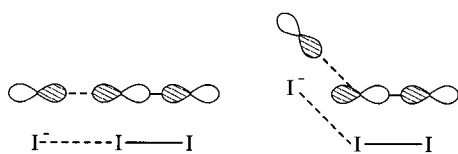
Based upon this energy decomposition, the electrostatic forces in I_3^- seem to be ten times stronger than the net orbital interaction. Does this mean that orbital interactions are unimportant in the trihalides or that electrostatic forces control the interactions? We believe that, while there are strong electrostatic interactions between the I^- and the I_2 components, important orbital factors are also at work.

Recall that the orbital interaction which stabilizes I_3^- occurs between I^- p_{σ} and I_2 4 σ . Without the partial population of some unoccupied (in the fragment) orbital, the net orbital energy in the closed shell–closed shell interaction between I^- and I_2 would consist almost entirely of the unfavorable Pauli repulsion. In this system, the only reasonably low-lying unoccupied orbital available (the higher principal quantum number orbitals on I are not members of this set) is 4 σ on I_2 .

In experimentally observed structures I_3^- is linear or near linear. This evidence actually demonstrates how important orbital interactions are to the structure of I_3^- . A sketch of the p_{σ} orbital on an I^- interacting with an I_2 4 σ is shown in 7. The left side indicates that the I^- p_{σ} and I_2 4 σ orbitals are pointed directly at each other (maximizing their overlap) in the linear geometry. While the bending distortion does increase the overlap between the p_{σ} orbital on the I^- and the iodine π system,

Table 1 Complete results for ADF calculations on the trihalides: E_{oi} is the orbital interaction energy, Occ(LUMO of X_2) the calculated occupation of the LUMO of the X_2 fragment, $Q(X_{term})$ and $Q(X_{cent})$ are the calculated charges on the terminal and central atoms, respectively

	I_3^-	Br_3^-	Cl_3^-	F_3^-
$R(X-X)/\text{\AA}$	3.14	2.64	2.37	1.77
Bonding $E/\text{kcal mol}^{-1}$	37.5	39.6	39.1	48.3
$E_{Pauli}/\text{kcal mol}^{-1}$	51.4	73.3	81.3	68.0
$E_{\text{elstat}}^*/\text{kcal mol}^{-1}$	-44.3	-56.6	-51.1	-38.7
$E_{oi}^*/\text{kcal mol}^{-1}$	-55.8	-71.0	-82.5	-106.6
Occ(LUMO of X_2)	0.57	0.58	0.58	0.58
$Q(X_{term})$	-0.419	-0.415	-0.419	-0.412
$Q(X_{cent})$	0.163	-0.169	-0.162	-0.177



7

this does not provide any stabilization since there are no unoccupied π orbitals on I_2 .

To probe the orbital control of the geometry of I_3^- a numerical experiment was carried out. The I^- was rotated relative to the I_2 (as in 7) to an I-I-I angle of 120° . The I-I distances were held fixed at 3.14 \AA . This distortion causes the I^-I_2 bonding energy to decrease by 19.7 kcal mol^{-1} . The majority of this decrease is in the orbital interaction term, which goes down by 21.5 kcal mol^{-1} upon bending. This is partially offset by a small 2.5 kcal mol^{-1} decrease in the Pauli repulsion. The electrostatic attraction changes only a tiny amount (decreasing by 0.7 kcal mol^{-1}). So, while the linear geometry of I_3^- is determined by orbital interactions, the majority of the I^-I_2 bond energy arises from electrostatic effects.

The computational results for all trihalides are summarized in Table 1. All four trihalide anions possess symmetric structures. In all of the trihalides the X-X bond lengths are approximately 0.3 \AA longer than in the corresponding dihalide (the ADF-optimized bond lengths of the diatomics are I_2 2.86, Br_2 2.36, Cl_2 2.04, F_2 1.42 \AA). This near-constant stretching upon complexation represents a larger and larger fraction of the X-X distance as we move from $I \rightarrow Br \rightarrow Cl \rightarrow F$. At the same time, the X-X bond strength increases upon moving from $I \rightarrow Br \rightarrow Cl$ and then drops at F (experimental values for the bond enthalpies are,⁵² in kcal mol^{-1} : I_2 36.1, Br_2 46.1, Cl_2 57.8, F_2 37.0). So, while the net interaction energy increases upon moving along this series, the preparation energy (the energy required to stretch X_2 to the X-X distance found in X_3^-) also increases. The net effect is little change in the bonding energy. These trends are easily visible in Fig. 4.

Our calculated X^-X_2 bonding energies are in excellent agreement with previously published pseudo-potential valence-bond results (I_3^- 35.7, Br_3^- 39.2, Cl_3^- 39.0 kcal mol^{-1}),⁷ and in reasonable agreement with other published DFT results (I_3^- 28.1, Br_3^- 38.0, Cl_3^- 39.7, F_3^- 47.3 kcal mol^{-1}),¹³ but they differ significantly from the results of second-order Møller-Plesset perturbation (MP2) calculations (I_3^- 28.1, Br_3^- 25.9, Cl_3^- 19.4, F_3^- -23.6 kcal mol^{-1}).¹⁰ Unfortunately, we are not aware of any measurements of these values in the gas phase. The 'standard' value reported for the bond strength in I_3^- , 24.0 kcal mol^{-1} , was derived from solution-phase electrochemical methods.⁵³ While it is tempting to argue that I_3^- must be the most stable of the X_3^- ions because it is the most stable in aqueous solution and is observed far more frequently in solid-state structures, these facts cannot necessarily be used to construct an argument about the gas-phase bond strengths. It is

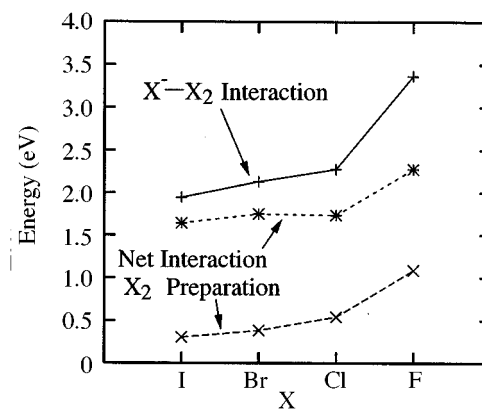


Fig. 4 Important energy terms in the X^-X_2 interaction. The net interaction energy shown here is the X^-X_2 bonding energy without BSSE or ZPE corrections

very likely that the stability ordering of the trihalides in aqueous solution is heavily influenced by the solvation energy of the X^- .⁷ There is also evidence that the stability ordering reverses in some non-aqueous solvents.⁵⁰ The lack of a reliable gas-phase measurement of the trihalide bond strengths and the contradictory solution-phase data makes it difficult to decide which set of theoretical bond energies is more accurate.

Before moving on, it is instructive to point out that the potential energy surfaces for X-X bond stretching in these trihalides are very flat, particularly in the case of I_3^- . In a 'numerical experiment' where the I^-I_2 bond length was varied by 0.3 \AA to either side of the minimum energy value while the I-I bond was held fixed at 3.14 \AA , the maximum energy change was less than 5.8 kcal mol^{-1} (this is an upper limit on the true energy change since the I-I bond was not allowed to relax to minimize the energy). This very flat energy surface helps to explain the large range of X-X bond lengths seen in crystal structures of the trihalides:^{50,54-56} small perturbations arising from the counter ions in the crystal can cause significant distortions in the X_3^- anions.

The Mixed Trihalide Anions: IIX^- and IXI^-

Next we will examine the effects of an electronegativity perturbation on I_3^- , that is the substitution of one of the I atoms by a more electronegative halide, X (Br or Cl). There are two possible substitution sites in I_3^- , the central atom (giving IXI^-), or the terminal atom (giving IIX^-). We will analyse the bonding and energetics for both substituted structures.

Within the framework of qualitative MO theory, we would expect the more electronegative atom to prefer the site with greatest electron density in the unperturbed system. Recall that our calculations on the homoatomic trihalide anions, as well as the qualitative MO view of the bonding in the trihalides, show that the negative charge in these anions is concentrated on the terminal atoms. So we would expect the IIX^- geometry, where the more electronegative X is in a terminal position, to be favored over IXI^- .

We approach the analysis of these systems by considering the bonding of I^- to an IX molecule. The I^- can bond either to the I, giving IIX^- , or to the X, giving IXI^- . In our donor-acceptor view, I^- is the donor and the IX is the acceptor. In thinking of site preferences for a donor attacking an acceptor there are two approaches which can be used. The first of these, called orbital control, argues that the donor will prefer to attack the site where it experiences maximum overlap interaction (thus, overlap) with a specific acceptor orbital. In the case of IX, the unoccupied σ^* level is localized more on the less electronegative I atom, so the orbital-control argument leads us to predict that I^- attack at the I of IX will be favored. The second approach, charge control, focuses not on the frontier orbitals

Table 2 Complete results for ADF calculations on the mixed halides: $R(X^1-X^2)$ is the distance between the leftmost and central atoms, $R(X^2-X^3)$ that between the central and rightmost atoms, E_{oi} is the orbital interaction energy, Occ(LUMO) the calculated occupation of the LUMO of the X_2 fragment and $Q(X^{1-3})$ the calculated charge on the corresponding atom

	IICl ⁻	IClI ⁻	IIBr ⁻	IBrI ⁻
$R(X^1-X^2)/\text{\AA}$	3.11	2.80	3.14	2.91
$R(X^2-X^3)/\text{\AA}$	2.66	2.80	2.84	2.91
Bonding $E/\text{kcal mol}^{-1}$	37.0	28.5	36.6	33.6
$E_{\text{Pauli}}/\text{kcal mol}^{-1}$	53.1	59.1	50.6	59.7
$E_{\text{elstat}}/\text{kcal mol}^{-1}$	-48.7	-33.9	-48.0	-46.2
$E_{oi}/\text{kcal mol}^{-1}$	-52.0	-69.6	-52.4	-64.9
Occ(LUMO)	0.52	0.67	0.54	0.63
$Q(X^1)$	-0.453	-0.378	-0.442	-0.391
$Q(X^2)$	-0.119	-0.243	-0.136	-0.218
$Q(X^3)$	-0.428	-0.378	-0.423	-0.391

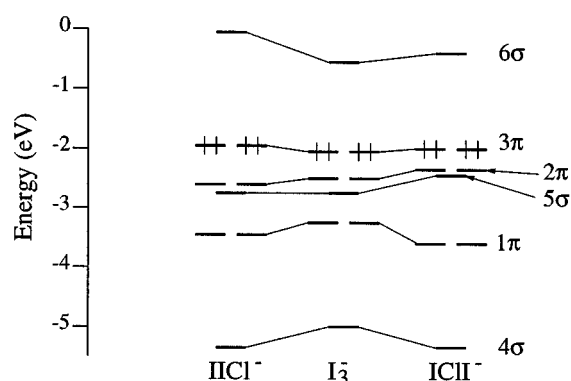


Fig. 5 A 'correlation diagram' for the 'conversion' of I_3^- into $IICl^-$ and $IClI^-$. In all cases the energy levels are those for the anions in their optimized geometries

but on the net charge asymmetries in the acceptor molecule. It argues that the negatively charged donor will prefer to approach the site with least negative charge. Once again, in IX this corresponds to the less electronegative I atom. In this case, both orbital- and charge-control arguments lead us to the same conclusion reached above using the electron-rich three-center MO scheme.

When an I^- bonds to an ICl atom through the I atom to give $IICl^-$ the calculated bonding energy is $37.0 \text{ kcal mol}^{-1}$ (geometrical details are given in Table 2). Bonding of I^- at the Cl atom to give $IClI^-$ leads to a bonding energy of only $28.5 \text{ kcal mol}^{-1}$. These results fit in quite neatly with our expectations.

Before moving on to the discussion of I^- attacking IBr (where the results fit less tidily into our qualitative scheme), let us first try to understand the bonding in $IICl^-$ and $IClI^-$ in greater detail. Fig. 5 treats the Cl-containing anions as electronegativity perturbations of I_3^- and shows the changes in MO energies in the form of a correlation diagram. Both $IICl^-$ and $IClI^-$ have orbital splitting patterns similar to that of I_3^- . Once again we focus on the σ system since the π orbitals of these electron-rich anions are completely occupied and do not play an important role in determining the behavior of the molecules.

The orbitals of the symmetric $IClI^-$ anion, not shown, are very similar to those of I_3^- shown in Fig. 2. This must be the case, as the shapes of these orbitals is determined by the symmetry of the molecule. An I-Cl bond is significantly stronger than an I-I bond (the experimental values of the bond enthalpies of the neutral molecules are $36.1 \text{ kcal mol}^{-1}$ for I_2 and $50.2 \text{ kcal mol}^{-1}$ for ICl^{52}). So the 4σ level of $IClI^-$ is lower in energy than the 4σ orbital of I_3^- . Similarly, $IClI^- 5\sigma$, which is weakly I-Cl antibonding, is higher in energy than $I_3^- 5\sigma$. Similar considerations apply to $IICl^-$, though the asymmetry present changes the shape of the orbitals (particularly 5σ) a small amount.

We next examine the energy decomposition for the I^- -ClI and I^- -ICl interactions in order to track down the reasons for the preferred attack of the I^- at the I. The difference in Pauli repulsion, which contributes $53.1 \text{ kcal mol}^{-1}$ in $IICl^-$ and $59.1 \text{ kcal mol}^{-1}$ in $IClI^-$, most likely arises primarily within the σ system. In ICl the highest occupied σ orbital, 3σ , has a larger contribution from the Cl atom than from I (the orbital is 57% Cl). This leads to increased interaction between 3σ and p_o when the I^- bonds through the Cl. Since both orbitals are occupied this larger interaction leads to more Pauli repulsion.

The difference in the orbital interaction energies between the two geometries ($-69.6 \text{ kcal mol}^{-1}$ for $IClI^-$ vs. $-52.0 \text{ kcal mol}^{-1}$ for $IICl^-$) can be understood by considering the amount of charge transfer and polarization which takes place upon forming the molecules from I^- and ICl fragments. As discussed above, the central atom of the electron-rich linear triatomic is the least negatively charged. In ICl, the Cl atom, due to its great electronegativity, has a partial negative charge. Owing to this, a great deal of charge redistribution in the ICl fragment must take place to lessen the charge on the Cl atom when $IClI^-$ is formed. This polarization shows up in the orbital interaction energy term. When I^- attacks at the I side of ICl less charge redistribution takes place and the orbital interaction term is smaller. The differences in orbital interaction strength are reflected in the occupation of the LUMO of ICl, which is almost 30% higher in $IClI^-$ than in $IICl^-$ (recall that population of the LUMO of the acceptor is the only available route for electron transfer in these species).

When we consider the *net* orbital interaction term (the sum of the Pauli and orbital interactions), I^- attack at the Cl of ICl to form $IClI^-$ is favored over attack at the I to form $IICl^-$ by $6.0 \text{ kcal mol}^{-1}$. The deciding factor in the total energy is the electrostatic contribution. In ICl the more electropositive I atom carries a partial positive charge (the charge on I is $+0.106$). Thus I^- attack at the partially positive I is more electrostatically favorable than attack at the partially negative Cl. The difference in electrostatic energies between the two geometries (the $IICl^-$ geometry is favored by $14.8 \text{ kcal mol}^{-1}$) is large enough to counter the orbital preference for the formation of $IClI^-$. Once again, though the primary contribution to the total bonding energy is electrostatic, orbital interactions play a major role in determining the geometry of the mixed trihalide anion, leading to the linear geometry for reasons already covered in the discussion of I_3^- .

The difference in energy between $IIBr^-$ and $IBrI^-$ is less pronounced (the difference is only 3.0 compared with $8.5 \text{ kcal mol}^{-1}$ in the Cl-containing system). This is despite the fact that the differences in Pauli repulsion and orbital interaction follow the same trends as in the chloride anions (shown in Table 2). The difference is that the electrostatic contributions to the bonding energies of the two geometries are very similar. This is due almost entirely to the fact that IBr is considerably less polarized than ICl (the charge on I in IBr is only $+0.066$), since Br is less electronegative than Cl.

The small difference in I-IBr bonding energies between $IIBr^-$ and $IBrI^-$ leads us to expect that a mixture of IBr and I^- in the gas phase would lead to the production of both trinuclear isomers. Judging from the importance of solvation in X_3^- stabilities, the relative stabilities of $IBrI^-$ and $IIBr^-$ in condensed phases (solution or a crystal) may differ significantly from our predictions for the gas-phase values. At least one compound containing an $IBrI^-$ anion has been structurally characterized.⁵⁷ When used as a counter ion for 4,5-ethylenedithio-4',5'-(2-oxatrimethylenedithio)diselenadithiafulvalene, the $IBrI^-$ anion is linear and centrosymmetric with 2.89 \AA I-Br bond lengths.

Hypervalent Bonding in the Hydrogen Bihalide Anions: XXH^- and XXH^-

We now shift gears and examine a related but separate class of

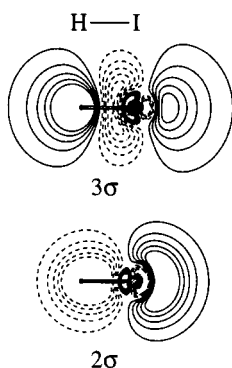
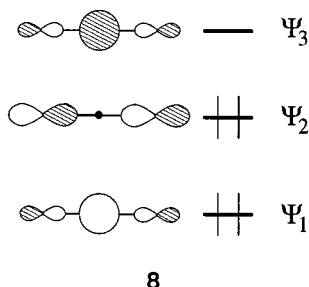


Fig. 6 The important valence σ orbitals of HI: 2σ , the highest occupied orbital in the σ system and 3σ , the LUMO of the molecule



hypervalent compounds: the hydrogen bivalides. They have stoichiometry HXY^- ($X, Y = \text{F, Cl, Br or I}$), with the H atom located on the line between the two halogens. Here we only examine the homoatomic hydrogen bivalides ($X = Y$). These anions are typically considered to be examples of 'strong hydrogen bonding'.^{3,58} Our intention is to show that the bonding in these compounds can be explained quite satisfactorily in terms of both hypervalency (the two-co-ordinate H is formally hypervalent) and donor-acceptor interactions. While this analysis will focus on the XHX^- anions, in line with the previous sections we will briefly discuss the XXH^- species.

When we consider the $1s$ orbital on the H and the valence p_z orbitals on the halides, XHX^- is another three-orbital system. Since the H atom can interact solely through its $1s$ orbital, the qualitative orbital scheme for the bonding is slightly different from that in the trihalides. The new three-orbital picture is shown in **8**. This system shares with **1** the following features: Ψ_1 is X-H bonding, Ψ_2 is non-bonding, and Ψ_3 is X-H antibonding. Again the levels are occupied through Ψ_2 .

We start our discussion of the bonding in the symmetric hydrogen bivalides with IHI^- . Once again the optimized geometry of the anion is symmetric, with H-I distances of 1.99 \AA (0.34 \AA longer than the optimized distance in HI). The energy decomposition was performed using HI and I^- as fragments.

Based on the similarity between **1** and **8** we will analyse the bonding in IHI^- in terms of donor-acceptor bonding. The important σ orbitals of HI for the donor-acceptor bond are, once again, the highest occupied σ level (2σ) and lowest unoccupied σ orbital (3σ , which is the LUMO of HI). Contour plots of these two orbitals are shown in Fig. 6. The 2σ orbital of HI is H-I bonding, and consists of 36% H $1s$, 13% I $5s$ and 49% I $5p_z$. The orbital is localized primarily on the more electronegative element: I. The antibonding 3σ orbital has a larger contribution from the hydrogen atom (65%).

An FMO interaction diagram for the bonding of I^- through the H of HI is shown in Fig. 7. We observe a very small splitting between the 1π and 2π orbitals. This is because the H atom does not have any valence orbitals of π symmetry and the I atoms are very far (almost 4 \AA) apart, so they only interact weakly. There are π symmetry polarization functions on the H, but these only interact to a small degree, contributing a mere

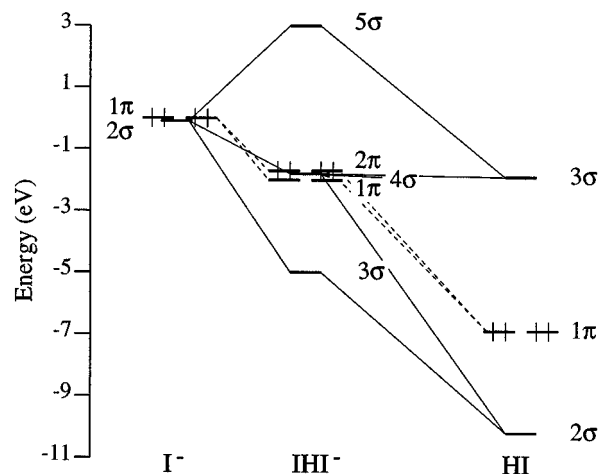


Fig. 7 Fragment molecular orbital (FMO) interaction diagram for IHI^- . The symmetry labels given are appropriate for the C_{2v} symmetry within which the calculation was performed. Solid lines connect levels of σ symmetry, dashed lines connect levels of π symmetry

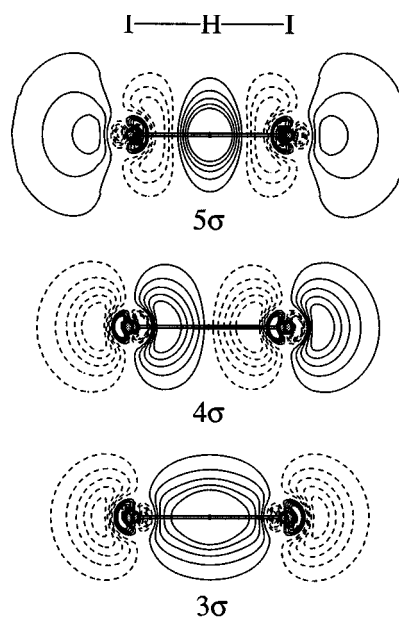


Fig. 8 Contour plots of the valence σ orbitals of IHI^-

1.1% to the 1π orbital. The I^- -HI interactions occur almost exclusively through the σ system.

Contour plots of the three valence σ orbitals of IHI^- , 3σ , 4σ and 5σ , are shown in Fig. 8. The σ orbitals in this hypervalent compound match the qualitative prediction (**8**) very nicely. These orbitals are occupied up through the I-H non-bonding/I-I antibonding 5σ .

The analysis of the bonding in IHI^- in the language of donor-acceptor interactions is more or less identical to that used earlier in our discussion of the bonding in I_3^- , so we will not repeat much of it here. The acceptor level on the HI fragment (3σ) is again heavily mixed into the highest occupied σ orbital of IHI^- , 4σ . This partial occupation of 3σ (the occupation is 0.52) is responsible for the charge transfer from I^- to HI on formation of IHI^- .

The calculated data for all of the symmetric hydrogen bivalides are collected in Table 3. As we move along the series from HI to HF and the electronegativity of the halogen increases, the charge polarization (dipole moment) in the HX molecule goes up and the H atom becomes more and more positively charged. The calculated values of the dipole moments, HI 0.64, HBr 0.79, HCl 1.03 and HF 1.75 D, compare very well with the experimental values, HI 0.42, HBr 0.80, HCl 1.08 and HF 1.91 D.⁵² This rising polarization increases

Table 3 Results for ADF calculations on the hydrogen bihalides: E_{oi} is the orbital interaction energy, Occ(LUMO) the calculated occupation of the LUMO of the HX fragment, $Q(X)$ and $Q(H)$ are the calculated charges on X and H

	IHI ⁻	BrHBr ⁻	ClHCl ⁻	FHF ⁻
$R(X-H)/\text{\AA}$	1.99	1.74	1.60	1.16
Bonding $E/\text{kcal mol}^{-1}$	20.9	25.5	29.8	47.9
$E_{\text{Pauli}}/\text{kcal mol}^{-1}$	57.2	62.1	62.7	68.6
$E_{\text{elstat}}^*/\text{kcal mol}^{-1}$	-25.1	-34.2	-42.0	-78.3
$E_{oi}^*/\text{kcal mol}^{-1}$	-62.0	-65.2	-66.2	-64.4
Occ(LUMO)	0.52	0.46	0.42	0.17
$Q(X)$	-0.480	-0.487	-0.494	-0.503
$Q(H)$	-0.039	-0.027	-0.011	0.005

the electrostatic interaction with the approaching X^- anion. In the optimized geometries of XHX^- , E_{elstat}^* increases nearly linearly with the calculated charge on the H atom in the optimized geometry of HX.

While both the Pauli repulsion and orbital energies increase along the series of halides (with the exception of the orbital term for FHF⁻, which is lower than for either BrHBr⁻ or ClHCl⁻), the sum of the two terms (the net orbital interaction) does not change significantly. Thus, the major factor driving the bonding strength trend in the hydrogen bihalide series is the change in electrostatic energies brought about by the increasing electronegativity of the halogen as we move from I \rightarrow F.

Though the trends in bonding strength in the hydrogen bihalide anions are driven by electrostatics as we move along the series I \rightarrow Br \rightarrow Cl \rightarrow F, it is important to realize that there are both significant orbital contributions to the bonding energy and sizable charge transfers from X^- to HX. Once again, the bonding is not purely electrostatic. The results show that strong hydrogen bonds can be understood in terms of both hypervalent bonding through the hydrogen atom and donor-acceptor interactions between X^- and HX.

Our theoretical results are in very good agreement with both the experimental and theoretical data reviewed by Klepeis *et al.*⁵⁹ Compared to the experimental data, the ADF bonding energies are consistently high by 3–9 kcal mol⁻¹ (the disagreement with experiment increases along the series I \rightarrow F). The calculated bond lengths are all too long by less than 0.1 Å.

Just as in the case of the mixed trihalide anions, X^- attack at the X side of HX was explored. In these unlikely geometries an electronegative X atom is located in the central (least negatively charged) position, while the relatively electropositive H atom is in one of the terminal positions. While the results of these calculations will not be presented in any great depth here, the bonding energies are significantly lower (as expected) and decrease upon moving from I to F: HII⁻ 5.4, HBrBr⁻ 4.5, HClCl⁻ 2.0 kcal mol⁻¹, HFF⁻ no bonding. The electrostatic interactions which stabilized the XHX^- anions are drastically reduced in these anions, since the I^- is attacking at a site which is already electron-rich. This effect grows more pronounced as the charge on the halogen being attacked grows, so the bonding energy decreases as we increase the electronegativity of X. In addition, the Pauli repulsion in the XXH^- anions plays a far more important role in the final energetics. In XHX^- the π orbitals of the attacking X^- do not interact significantly with the HX, so their contribution to the Pauli repulsion is most likely quite small (again, we cannot present numbers for this since ADF does not permit symmetry decomposition of the Pauli repulsion). However, when the X^- attacks the X side of HX there is a significant amount of repulsion arising due to interactions between the p_π orbitals on the two X atoms. Both the electrostatic and Pauli terms indicate that the HXX^- anions are not likely to be particularly stable.

A reviewer has pointed us to a possible extension of this bonding scheme to $X-M-X^-$ with $M = Cu, Ag$ or Cu . These anions are experimentally well known, for example: $Cs_2[M^I-$

$Cl_2][Au^{III}Cl_4]$ ($M = Au$ or Ag) have linear $CIMCl^-$ units, and $ClCuCl^-$ has been observed when $CuCl$ is dissolved in HCl .⁶⁰ The difference in these systems, or for that matter, in the neutral $X-M-X$ ($M = Zn, Cd$ or Hg) species is that the central atom possesses low-lying mp orbitals. This allows the formation of two strong, 'localized' $M-X$ bonds.

Conclusion

We have shown that the nature of the bonding in the trihalides, mixed trihalides, and hydrogen bihalides can be viewed as either electron-rich three-center or donor-acceptor bonding. The results of the density-functional calculations support the 'classical' view of hypervalent bonding put forth by Pimentel and Rundle: the p_σ system of X_3^- consists of one bonding, one non-bonding, and one antibonding MO. The first two of these orbitals are occupied. This analysis explains the bonding in these anions without including unoccupied d orbitals on the central atom.

The bonding in X_3^- , X_2Y^- and XHX^- can also be viewed as a donor-acceptor interaction between closed-shell fragments: X^- (the donor) and either X_2 , XY or HX (the acceptor). In this view the bonding is due to interactions between the occupied p_σ orbital of the donor and the σ^* LUMO of the acceptor. These interactions give rise to both charge transfer from the donor to the acceptor and weakening of the bonding within the acceptor through partial occupation of a acceptor σ^* orbital. The formally non-bonding central orbital in the Pimentel-Rundle scheme derives from the donor orbital mixing with an occupied acceptor σ orbital in an antibonding way, and with an unoccupied acceptor σ^* orbital in a bonding way.

The Transition State energy decomposition procedure used indicates that it is very difficult to assign responsibility for the bonding in these hypervalent anions to any particular energy term. Using our definition of a 'net orbital' energy (the sum of the Pauli and orbital interaction terms of the TS procedure), we found that, on first glance, the dominant energy term in the bonding is the electrostatic contribution. This is not, however, the whole story. The linear geometries of the molecules are determined by orbital energy terms. On the other hand, the site preference for attack in the mixed trihalides (X versus Y attack on XY) and hydrogen bihalides (H versus X attack on HX) is driven by electrostatic terms. The story is not easily reduced to a single important factor.

It is likely that this type of analysis, which unifies the bonding picture for the 'hypervalent' bonding in trihalides and 'strong hydrogen bonding' in hydrogen bihalides, can be extended to look at the bonding in more complicated electron-rich molecules, weak closed shell-closed shell intermolecular interactions, and, possibly, intermolecular hydrogen bonding. We are currently in the process of applying this donor-acceptor/hypervalency analysis to an investigation of the nature of 'secondary bonds', intermolecular contacts in a crystal which are intermediate in length between covalent and van der Waals contacts,⁶¹ and to the bonding in a number of R_2QX_2 ($Q = Se$ or Te ; $X = I, Br$ or Cl) compounds.

Acknowledgements

We are grateful to the National Science Foundation for its support of our work through Research Grant CHE 94-08455. We would also like to thank Silicon Graphics for their generous donation of the computer hardware which was used in this work.

References

- 1 L. Pauling, *The Nature of the Chemical Bond*, Cornell University Press, Ithaca, NY, 1st edn., 1940.
- 2 G. E. Kimball, *J. Chem. Phys.*, 1940, **8**, 188.

- 3 G. C. Pimentel, *J. Chem. Phys.*, 1951, **19**, 446.
- 4 R. J. Hach and R. E. Rundle, *J. Am. Chem. Soc.*, 1951, **73**, 4321.
- 5 R. Gleiter and R. Hoffmann, *Tetrahedron*, 1968, **24**, 5899.
- 6 E. F. Riedel and R. D. Willett, *Theor. Chim. Acta*, 1976, **42**, 237.
- 7 P. W. Tasker, *Mol. Phys.*, 1977, **33**, 511.
- 8 M. Kertész and F. Vonderviszt, *J. Am. Chem. Soc.*, 1982, **104**, 5889.
- 9 W. Kutzelnigg, *Angew. Chem., Int. Ed. Engl.*, 1984, **23**, 272.
- 10 J. J. Novoa, F. Mota and S. Alvarez, *J. Phys. Chem.*, 1988, **92**, 6561.
- 11 G. L. Gutsev, *J. Struct. Chem.*, 1990, **30**, 733.
- 12 L. H. Sæthre, O. Gropen and J. Slettern, *Acta Chem. Scand.*, 1988, **42**, 16.
- 13 G. L. Gutsev, *Russ. J. Phys. Chem.*, 1992, **66**, 1596.
- 14 T. G. Wright and E. P. F. Lee, *Mol. Phys.*, 1993, **79**, 995.
- 15 K. Yamashita, K. Morokuma and C. Leforestier, *J. Chem. Phys.*, 1993, **99**, 8848.
- 16 R. J. Gillespie and E. A. Robinson, *Angew. Chem., Int. Ed. Engl.*, 1996, **35**, 495.
- 17 D. Danovich, J. Hrušák and S. Shaik, *Chem. Phys. Lett.*, 1995, **233**, 249.
- 18 K. N. Robertson, P. K. Bakshi, T. S. Cameron and O. Knop, *Z. Anorg. Allg. Chem.*, 1997, **623**, 104.
- 19 C. A. Coulson, in *Hydrogen Bonding*, eds. D. Hadzi and H. W. Thompson, Pergamon, Oxford, 1959, p. 339.
- 20 K. Morokuma, *J. Chem. Phys.*, 1971, **55**, 1236.
- 21 K. Kitaura and K. Morokuma, *Int. J. Quantum Chem.*, 1976, **10**, 325.
- 22 K. Morokuma, *Acc. Chem. Res.*, 1977, **10**, 294.
- 23 H. Umeyama, K. Kitaura and K. Morokuma, *Chem. Phys. Lett.*, 1975, **36**, 11.
- 24 J. P. Foster and F. Weinhold, *J. Am. Chem. Soc.*, 1980, **102**, 7211.
- 25 A. E. Reed, R. B. Weinstock and F. Weinhold, *J. Chem. Phys.*, 1985, **83**, 735.
- 26 S. Shaik, H. B. Schlegel and S. Wolfe, *Theoretical Aspects of Physical Organic Chemistry: the S_N2 Mechanism*, Wiley, New York, 1992.
- 27 J. D. McCullough, *Inorg. Chem.*, 1964, **3**, 1425.
- 28 C. Knobler and J. D. McCullough, *Inorg. Chem.*, 1968, **7**, 365.
- 29 S. Akabari, Y. Takanohashi, S. Aoki and S. Sato, *J. Chem. Soc., Perkin Trans. 1*, 1991, 3121.
- 30 S. M. Godfrey, C. A. McAuliffe, R. G. Pritchard and S. Sarwar, *J. Chem. Soc., Dalton Trans.*, 1997, 1031.
- 31 N. Bricklebank, S. M. Godfrey, A. G. Mackie, C. A. McAuliffe, R. G. Pritchard and P. J. Kobryn, *J. Chem. Soc., Dalton Trans.*, 1993, 101.
- 32 N. Bricklebank, S. M. Godfrey, C. A. McAuliffe and R. G. Pritchard, *J. Chem. Soc., Dalton Trans.*, 1993, 2261.
- 33 N. Bricklebank, S. M. Godfrey, H. P. Lane, C. A. McAuliffe, R. G. Pritchard and J. M. Moreno, *J. Chem. Soc., Dalton Trans.*, 1995, 2421.
- 34 N. Bricklebank, S. M. Godfrey, A. G. Mackie, C. A. McAuliffe and R. G. Pritchard, *J. Chem. Soc., Chem. Commun.*, 1992, 355.
- 35 S. M. Godfrey, D. G. Kelly, C. A. McAuliffe, A. G. Mackie, R. G. Pritchard and S. M. Watson, *J. Chem. Soc., Chem. Commun.*, 1991, 1163.
- 36 N. Goldberg, G. A. Landrum and R. Hoffmann, unpublished work.
- 37 E. J. Baerends, D. E. Ellis and P. Ros, *Chem. Phys.*, 1973, **2**, 41.
- 38 E. J. Baerends and P. Ros, *Chem. Phys.*, 1975, **8**, 412.
- 39 E. J. Baerends and P. Ros, *Int. J. Quantum Chem.*, 1978, **S12**, 169.
- 40 A. D. Becke, *J. Chem. Phys.*, 1986, **84**, 4524.
- 41 A. D. Becke, *Phys. Rev. A*, 1988, **38**, 3098.
- 42 J. P. Perdew, *Phys. Rev. B*, 1986, **33**, 8822.
- 43 J. P. Perdew, *Phys. Rev. B*, 1986, **34**, 7406.
- 44 J. G. Snijders, E. J. Baerends and P. Vernoojis, *At. Data Nucl. Data Tables*, 1982, **26**, 483.
- 45 A. Rosa, A. W. Ehlers, E. J. Baerends, J. G. Snijders and G. te Velde, *J. Phys. Chem.*, 1996, **100**, 5690.
- 46 F. L. Hirshfeld, *Theor. Chim. Acta*, 1977, **44**, 129.
- 47 G. A. Landrum, YAEHMOP, yet another extended Hückel Molecular Orbital Package (freely available on the World Wide Web at: <http://overlap.chem.cornell.edu:8080/yaehmop.html>), 1995.
- 48 T. Ziegler, in *Metal-ligand interactions: from atoms, to clusters, to surfaces*, eds. D. R. Salahub and N. Russo, Kluwer, Dordrecht, 1992, p. 367.
- 49 T. A. Albright, J. K. Burdett and M.-H. Whangbo, *Orbital Interactions in Chemistry*, Wiley, New York, 1985.
- 50 A. J. Downs and C. J. Adams, *Comprehensive Inorganic Chemistry*, Pergamon, Oxford, 1976.
- 51 R. S. Drago, *Physical Methods in Chemistry*, Saunders College Publishing, Philadelphia, 1st edn., 1977.
- 52 P. W. Atkins, *Physical Chemistry*, W. H. Freeman, New York, 3rd edn., 1986.
- 53 L. E. Topol, *Inorg. Chem.*, 1971, **10**, 736.
- 54 A. F. Wells, *Structural Inorganic Chemistry*, Oxford University Press, New York, 5th edn., 1984.
- 55 P. K. Bakshi, M. A. James, T. S. Cameron and O. Knop, *Can. J. Chem.*, 1996, **74**, 559.
- 56 R. N. Robertson, T. S. Cameron and O. Knop, *Can. J. Chem.*, 1996, **74**, 1572.
- 57 T. Naito, A. Tateno, T. Udagawa, A. Kobayashi and T. Nogami, *J. Chem. Soc., Faraday Trans.*, 1994, 763.
- 58 J. Emsley, *Chem. Soc. Rev.*, 1980, **9**, 91.
- 59 N. E. Klepeis, A. L. East, A. G. Császár, W. A. Allen, T. J. Lee and D. W. Schwenke, *J. Chem. Phys.*, 1993, **99**, 3865.
- 60 N. N. Greenwood and A. Earnshaw, *Chemistry of the Elements*, Pergamon, New York, 1984.
- 61 N. W. Alcock, *Adv. Inorg. Radiochem.*, 1972, **15**, 1.

Received 29th May 1997; Paper 7/03736H